Available online at www.sciencedirect.com
ScienceDirect
Biochimica et Biophysica Acta 1757 (2006) 969–980
BIOCHIMICA ET BIOPHYSICA ACTA
BBA
www.elsevier.com/locate/bbabio

Review

Different types of biological proton transfer reactions studied by quantum chemical methods

Margareta R.A. Blomberg *, Per E.M. Siegbahn

Department of Physics, Stockholm Centre for Physics, Astronomy and Biotechnology (SC-FAB), Stockholm University, S-106 91 Stockholm, Sweden

Received 15 November 2005; received in revised form 20 December 2005; accepted 5 January 2006
Available online 25 January 2006

Abstract

Different types of proton transfer occurring in biological systems are described with examples mainly from ribonucleotide reductase (RNR) and cytochrome *c* oxidase (CcO). Focus is put on situations where electron and proton transfer are rather strongly coupled. In the long range radical transfer in RNR, it is shown that the presence of hydrogen atom transfer (HAT) is the most logical explanation for the experimental observations. In another example from RNR, it is shown that a transition state for concerted motion of both proton and electron can be found even if the donors are separated by a quite long distance. In CcO, the essential proton transfer for the O—O bond cleavage, and the most recent modelings of proton translocation are described, indicating a few remaining major problems.

Keywords: Quantum chemistry; Density functional theory; Cytochrome *c* oxidase; Proton transfer; Proton translocation

1. Introduction

Proton transfer reactions are important steps in almost all chemical reactions catalyzed by enzymes. Commonly, they are triggered by electron transfers of different types. These proton-coupled electron transfers can be separated into different groups depending on how strong the coupling is and how long range the electron transfer is. In one extreme, the proton and the electron will be transferred simultaneously from the same donor to the same acceptor. These reactions are usually referred to as hydrogen atom transfer (HAT) reactions. In the other extreme, an electron is transferred from a long distance in one direction while the protons move only a short distance in a completely different direction. All variants in between these extremes are also possible. In the present short review, examples of different types of proton transfer reactions will be described which have been encountered in quantum chemical studies of reaction mechanisms. It should here be mentioned that somewhat different theoretical approaches to describe coupled electron and proton transfer in biological systems can be found in the literature [1–3]. The examples in the present review will be taken mainly from two enzymes, Ribonucleotide Reductase (RNR) and Cytochrome *c* Oxidase (CcO). These enzymes have been chosen as examples since they provide a variety of different types of proton transfer reactions which have attracted large interest the past decade.

Ribonucleotide reductase consists of two proteins, R1 and R2, and catalyses the transformation of ribonucleotides into deoxyribonucleotides [4–6]. In RNR, there is a very interesting long range radical transfer over 30 Å between a donor in the R2 protein and an acceptor in R1, without any obvious redox centers in between. To explain how this transfer occurs, an unusually strongly coupled motion of protons and electrons has been suggested of a type not observed before or after in long range radical transfer in biology [7]. There are also other types of proton-coupled electron transfers in RNR of general interest, for example in the creation of the key tyrosyl radical and in the substrate reactions. A connection to photosystem II will be made since the tyrosyl reduction in RNR has stood as a model for the hydrogen atom transfer model of dioxygen formation in PSII [8].

Cytochrome *c* oxidase is the terminal enzyme in the respiratory chain and reduces molecular oxygen to water, using cytochrome *c* as the electron source [9–12]. The O_2 reduction is exergonic, and it is coupled to an endergonic proton

* Corresponding author.
E-mail address: mb@physto.se (M.R.A. Blomberg).

0005-2728/$ - see front matter © 2006 Elsevier B.V. All rights reserved.
doi:10.1016/j.bbabio.2006.01.002

transfer across the mitochondrial or bacterial membrane, building up a proton gradient, which eventually is used by ATP synthase to store the excess energy. Proton transfer across the membrane, usually termed proton translocation, is thus the goal for this enzyme. This is a very complicated process where for each proton consumed in the dioxygen chemistry there is one proton translocated. To accomplish this, protons initially travelling along the same path are required to go in different directions, for pumping or consumption, in different parts of the catalytic cycle. Gating mechanisms have been suggested leading the protons in the right direction and preventing them from going in the wrong direction. Examples of critical proton transfer reactions will be given from recent studies of both the activation of dioxygen and for the mechanism of proton translocation.

The theoretical method used in the studies discussed here is hybrid density functional theory (DFT) with the B3LYP functional [13]. This method was designed and fitted to data for first and second row elements, but has proven remarkably accurate also for transition metal complexes. Still, the relative accuracy for energies cannot be expected to be better than 3–5 kcal/mol. An essential part of theoretical studies of enzymes is obviously the design of an appropriate model [14]. The approach in the studies discussed here is to use a quantum chemical model as large as can be practically afforded, and to embed this model in a dielectric continuum. To keep the structure reasonably close to the X-ray geometries, some positions in the model are usually frozen from the experimental structure. The use of computational models has increased the last years to become a natural additional tool to investigate the details of enzymatic reactions, complementing the picture provided by experimental spectroscopic techniques. Quantum chemical computation is particularly useful for studying short-lived species and at present it is the only technique available that can provide structural and electronic details for transition states of chemical reactions in enzymes. In the description below, transition state structures will therefore be emphasized.

2. Coupled proton and electron transfer in RNR

Different types of mechanisms for proton coupled electron transfer in ribonucleotide reductase (RNR) have been intensely discussed the past decade. The enzyme is composed of two subunits, R1 where the substrate reactions take place, and R2 where an essential tyrosyl radical (Tyr122) is created, see Fig. 1. The distance between Tyr122 and the substrate is over 30 Å. The main point debated has been how the radical can move from Tyr122 to the substrate active site, without any obvious intermediate redox centers. A strongly coupled proton and electron transfer, referred to as hydrogen atom transfer (HAT), has been advocated for part of this transfer [7]. Another point of interest has been how the Tyr122 radical is generated through the oxidation of the iron dimer by dioxygen. Since the tyrosyl radical is known to be deprotonated, a main question has been how this deprotonation is coupled to electron transfer from tyrosine to the iron dimer. The mechanism suggested may again be termed HAT since the electron and proton come from the same donor and reach the same acceptor, even though the motion is not as strongly coupled as the radical transfer in the first example. A third example of proton coupled electron transfer discussed here, will be taken from the substrate reactions. In this case, long range electron transfer is coupled to a local proton transfer. In this rather common type of mechanism, the electron donor is not the same as the proton donor.

A striking feature of the X-ray structure of RNR is that Tyr122 and the substrate site are connected through a hydrogen bonding network (marked with a dashed line in Fig. 1). These hydrogen bonds turn out to be necessary for fast radical transfer. Experiments have shown that when Tyr730 or Tyr731 are mutated to phenylalanine the radical transfer stops [15]. This is the first time a single hydrogen bond has been shown to have such a dramatic effect on electron transfer, which suggests that an unusual type of mechanism is operative. It is not reasonable to explain this effect by a normal proton coupled electron transfer with a local proton donor other than the tyrosines. An explanation for the mutant experiment came with the realization that the radical transfer could partly involve a sequence of hydrogen atom transfer steps [7]. A requirement for an intermediate in an electron transfer is that it should be energetically reachable from the starting point. This requirement is obviously fulfilled by a tyrosyl radical in this case since the transfer starts out with such a radical. This means that the mechanism for electron transfer depends very much on the energy of the starting point. Electron transfer in water using the HAT mechanism would thus be very fast if a hydroxyl radical has first been created.

A typical HAT transition state is shown in Fig. 2 for a model of the two tyrosines in RNR. The barrier is only 5 kcal/mol which means that the rate is on the order of nanoseconds, almost competitive with that of pure electron transfer. At the TS, the spin is equally distributed on the tyrosines. It should be pointed out that in the HAT mechanism, there is never any spin on the hydrogen that moves, indicating that a strict literal interpretation of HAT should not be made. A similar TS can be located for HAT between Cys439 and Tyr730 with a barrier of 8 kcal/mol corresponding to a rate faster than microseconds. A characteristic general feature of the HAT mechanism is a very small solvent dependence, since there is hardly any charge separation. The estimated effect of the protein surrounding on the barrier is only a couple of tenths of a kcal/mol. A large part of the radical transfer in RNR can thus be explained by the presence of a HAT mechanism. This does not mean that the entire path involves HAT mechanisms. For example, in the region of the iron dimer a more complicated radical transfer has been suggested [14], more similar to the mechanism discussed next.

The Tyr122 radical in RNR is the first functional amino acid radical identified experimentally in an enzyme [16]. It is a very stable radical which can actually be stored for days. The creation of this radical has obviously attracted a large attention. The current understanding of the steps preceding the creation of this radical can be summarized as follows. The iron dimer first binds dioxygen as a peroxide in between the irons, in a *cis* μ-1,2 mode [17], forming a Fe (III,III)-complex. As the peroxide is

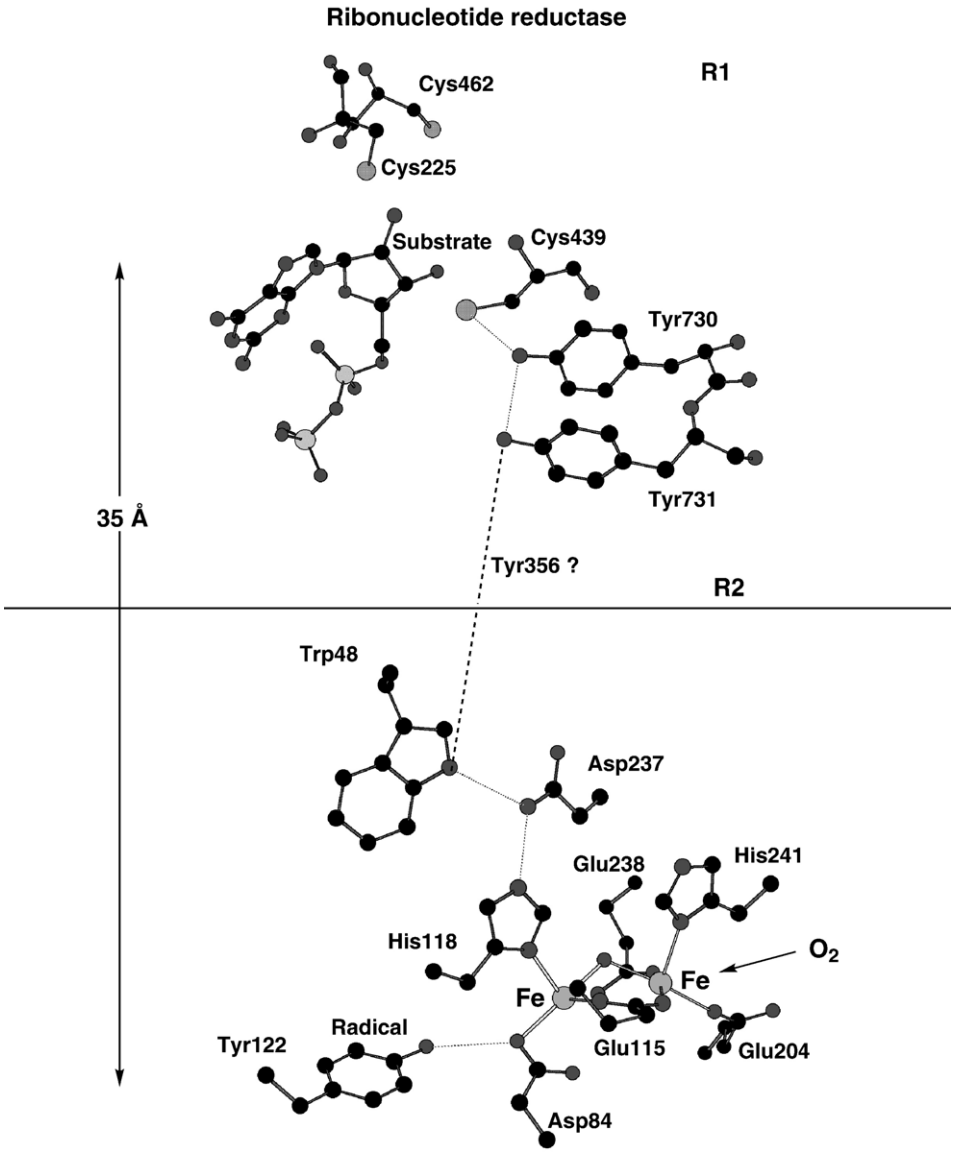

Fig. 1. X-ray structure of ribonucleotide reductase. The tyrosyl radical (Tyr122) is created in protein R2 while the substrate reactions occur in R1, 30 Å away.

cleaved an electron is transferred from Trp48 (see Fig. 1) to the dimer leading to a Fe_2 (IV,III)-complex termed compound *X*, which has two bridging unprotonated oxo groups [18]. The tyrosyl radical is created by reduction of compound *X* and at this stage a proton is taken up by one bridging oxo-group, leading to an iron dimer structure as shown in Fig. 3.

The creation of the tyrosyl radical has been studied by quantum chemical calculations [14], using a model as shown in Fig. 3. In this process, both an electron and a proton should be transferred from the tyrosine to the iron dimer. Since the distance between the iron dimer and tyrosine is fairly large, a water molecule has to be inserted to bridge this gap. In fact, without this water the computed barrier is far too high. An interesting transition state for transfer of both a proton and an electron was located as shown in Fig. 3. The spin on tyrosine has increased to 0.70 indicating that the electron transfer has proceeded more than halfways. The spin on one of the irons has decreased correspondingly. Interestingly, there is no spin on the atoms in between the iron dimer and tyrosine. Instead, this region shows the progress of proton transfer, which is about halfway at the TS. This type of proton coupled electron transfer has usually also been called HAT since the donor of the proton and the electron is the same (in this case tyrosine). If one regards the entire iron dimer complex as one unit, the acceptor is also the same. One could, of course, also choose to regard iron as the electron acceptor and a ligand as the proton acceptor, in which case the parallel to a pure HAT mechanism as in Fig. 2 is less clear. As usual, there is no spin on the hydrogen being transferred. The computed barrier for the tyrosyl radical formation is 10 kcal/mol, making this transfer quite rapid on the order of microseconds.

The reverse of the creation of the tyrosyl radical in RNR has stood as a model for the HAT-mechanism for dioxygen formation in PSII [8]. At the time this mechanism was suggested, there was no structure for PSII. As it later turned out, the distance between the oxygen evolving complex and the

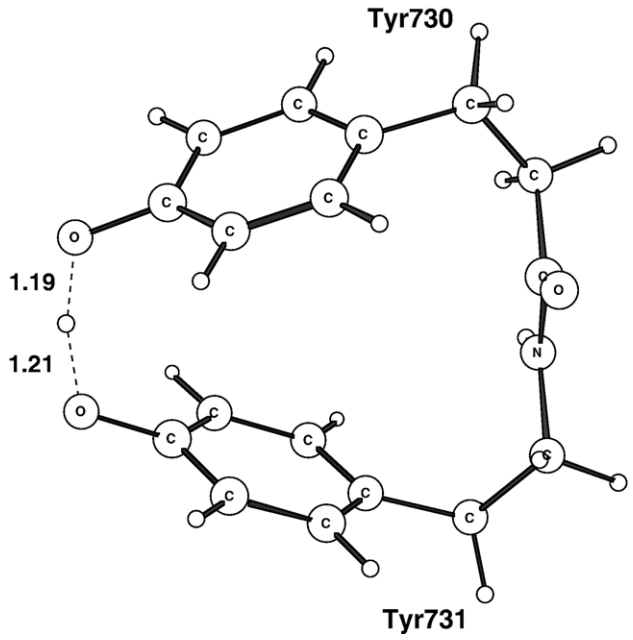

Fig. 2. Hydrogen atom transfer between Tyr730 and Tyr731 in RNR.

Tyr_Z radical in PSII is quite similar to the corresponding distance in RNR [19]. A calculation where iron is replaced by manganese in the model in Fig. 3 shows that this does not significantly affect the rate of the reaction, which is therefore in principle quite feasible also for PSII. However, there are other reasons to argue that a HAT mechanism is not likely for PSII, such as an unnecessary loss of oxidative power [20].

The final example of a proton coupled electron transfer process in RNR will be taken from the substrate reactions. The conversion of the substrate ribonucleotide to a deoxyribonucleotide is carried out in R1 with the Cys439 radical (see Fig. 1) as catalyst. In the suggested rate limiting step a ketoform of the substrate is converted to a protonated radical simultaneously with the formation of a disulfide bond between Cys225 and Cys462 [21], see Fig. 4. This means that a rather long range (about 8 Å) electron transfer from the cysteines to the substrate has to occur together with a proton transfer to the substrate from Glu441. It is computationally very demanding to locate such a transition state. In fact, it was far from clear that this type of TS could be found using DFT, since DFT suffers from the so called self-interaction error which tends to significantly overstabilize certain delocalized radicals [22]. When this happens, a TS can artificially turn into a stable species. However, in the present case a quite reasonable TS was eventually found as shown in Fig. 4. The concerted character of the electron and proton transfer events is clearly seen in the figure. The proton is in between the two oxygens of the substrate and Glu441, and the electron is delocalized with spins both on the substrate and the two cysteines 8 Å away. The calculated barrier is 19 kcal/mol which is slightly higher than the rate-limiting barrier of 17 kcal/mol for the substrate reactions. Normally, an error of this type of only a few kcal/mol does not prevent a decision on the most plausible mechanism. However, in the present case, there is a quite different mechanism, which assumes an additional proton in the model, which actually has a slightly lower barrier [23]. Detailed future comparisons between new experiments and theory are needed to decide which is the correct mechanism.

3. Proton transfer in cytochrome *c* oxidase, CcO

Cytochrome oxidase, located in the mitochondrial or bacterial membrane, is used here as an example to illustrate different types of processes where proton motion plays an essential role. The reduction of molecular oxygen to water in cytochrome oxidase occurs at the binuclear active site,

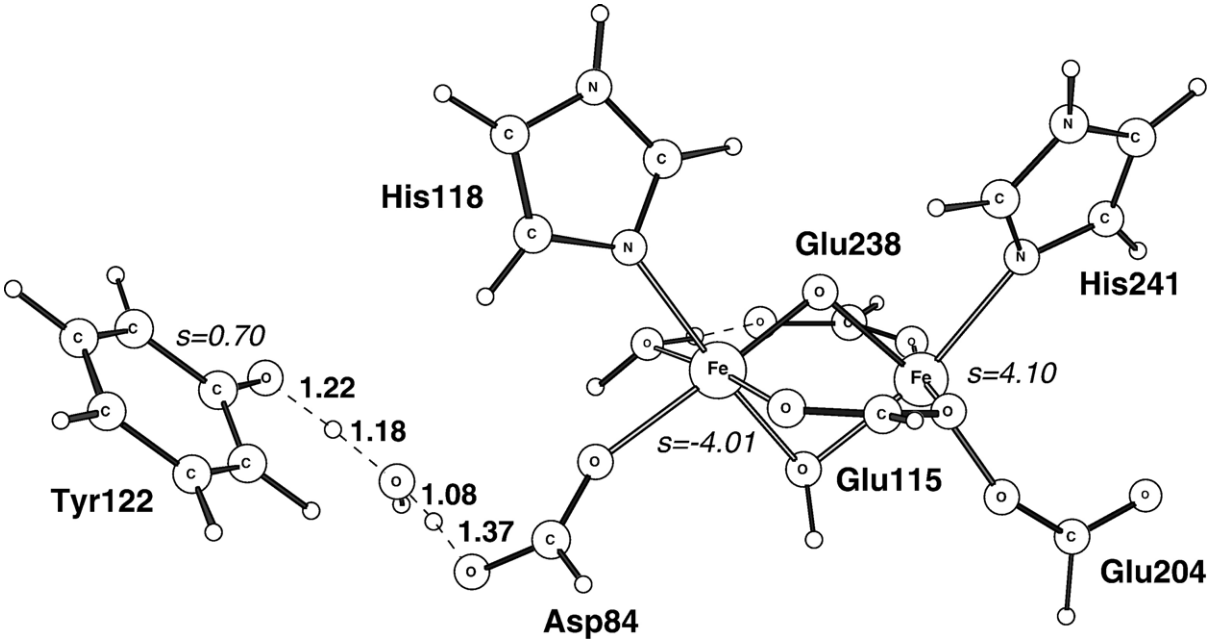

Fig. 3. Hydrogen atom transfer between tyrosine and compound X in RNR. Bond distances (Å) are given in bold and spins in italics.

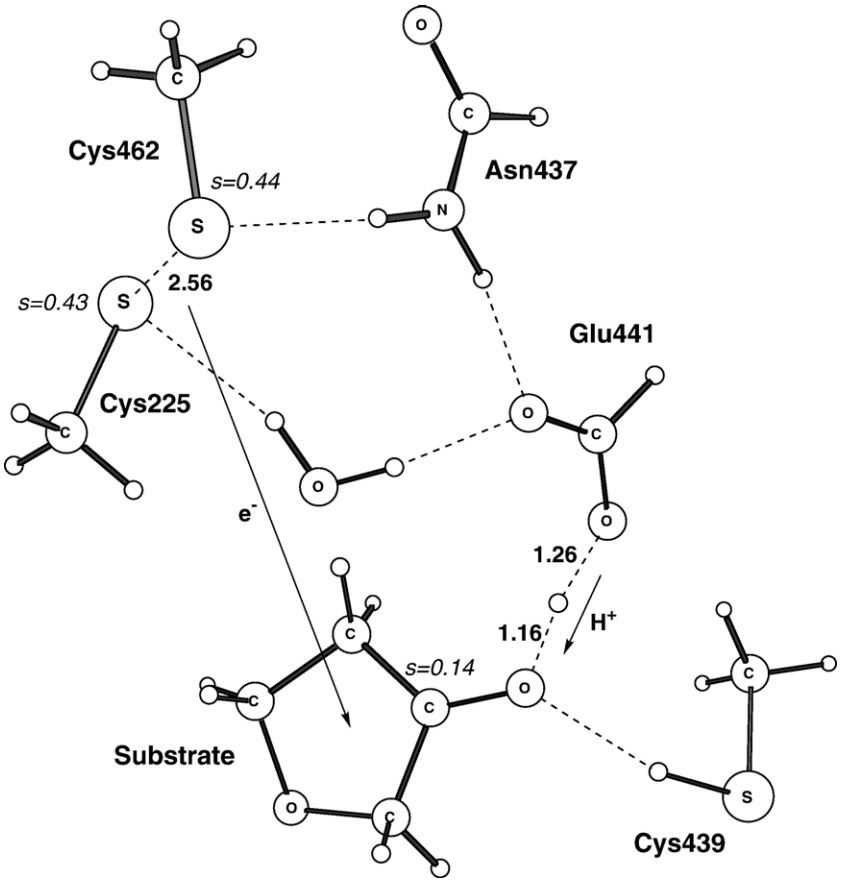

Fig. 4. Coupled proton and electron transfer in the substrate reactions of RNR. Bond distances (Å) are given in bold and spins in italics.

consisting of a heme group and a copper complex. The full reduction requires the uptake of four electrons from cytochrome *c* on the outside of the membrane, and four protons from the inside of the membrane. Coupled to this exergonic O_2 reduction, there is an endergonic translocation of four protons across the membrane [24], building up an electrochemical gradient that is used by ATP synthase to produce the energy-rich ATP molecules. The overall reaction can be written:

$$O_2 + 8H^+_{In} + 4^-_e \rightarrow 2H_2O + 4H^+_{Out}.$$

Proton motion in direct connection with the O−O bond cleavage step will first be described, followed by a discussion of proton uptake and translocation during the catalytic cycle.

3.1. Proton motion connected to O−O bond cleavage in CcO

Molecular oxygen coordinates to the reduced binuclear center, with Fe(II) and Cu(I). It has been shown that the O−O bond can be cleaved without any further transfer of electrons to the reduced binuclear center [25], and also that the O−O bond cleavage step is not connected to any uptake of protons from the inside of the membrane [26]. There is also some experimental evidence for the creation of a tyrosyl radical in this step [27]. To study this reaction step by density functional theory, a model of the binuclear center was built, as shown in Fig. 5. The model is built on the crystal structure of the bovine enzyme [28], with two water molecules added to make contact between the oxygen molecule and the tyrosine [29–31]. The calculations predict that the reaction proceeds via an unstable, not observable peroxide type of intermediate, where molecular oxygen is bridging between the two metals in the binuclear center, see Fig. 5. In this structure, two electrons have already been transferred to molecular oxygen, yielding Fe(III), Cu(II) and a bridging peroxide. The transfer of these first two electrons and the formation of the peroxide is not connected to any proton transfer. The negative charge on the oxygens is stabilized by the positively charged metal centers.

The remaining O−O σ-bond in the peroxide, on the other hand, cannot be cleaved without the transfer of a proton to the oxygen coordinating to copper, since otherwise the bond cleavage would lead to an oxo-group on copper, which is energetically very unfavorable. Therefore, the next step after the formation of the bridging peroxide, is the transfer of the proton from the tyrosine hydroxyl donor (**D**), via two water molecules in a Grotthuss type of mechanism, to the copper coordinating oxygen acceptor (**A**), see Fig. 6. This proton transfer is done in full without any electron transfer, and is fairly typical for proton transfer via several water molecules. In this case it leads to the formation of a Fe(III)–OOH compound coordinated to Cu(II) and a tyrosinate. The corresponding energy profile is shown in Fig. 7. In the present model, this proton transfer is found to be exothermic by 3 kcal/mol and the barrier is about 5 kcal/mol relative to the bridging peroxide [31]. It is found that this proton

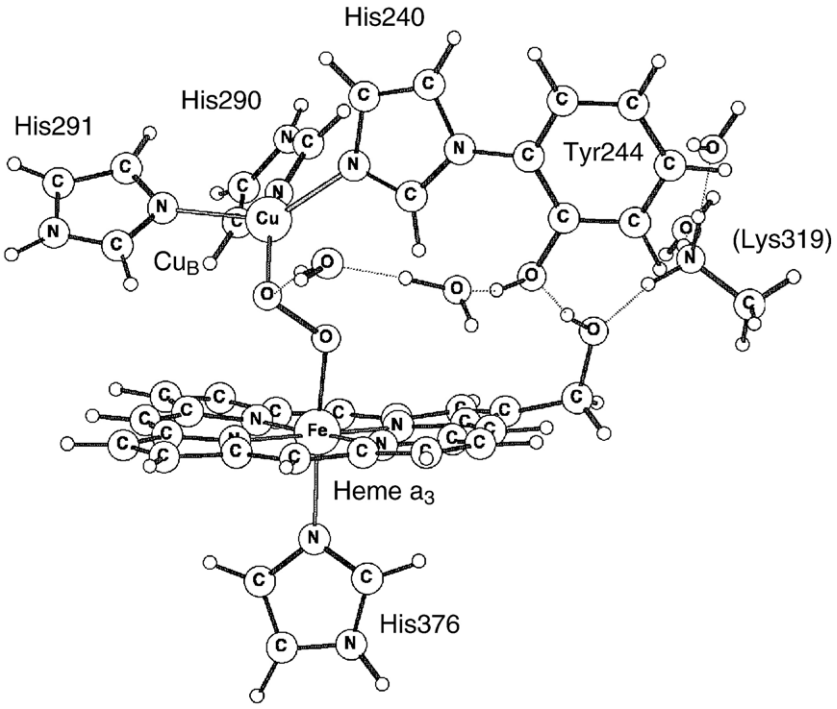

Fig. 5. Model of the binuclear center in CcO used in the calculations on the O−O bond cleavage step.

transfer is not a concerted process in the sense that all protons move at the same time, but rather a stepwise process with small energy differences between several different intermediate structures as indicated in the energy profile in Fig. 7. One of the intermediate structures on the proton transfer path, corresponding to the minimum with the highest energy, is shown in Fig. 6. It can be noted that the description of this process should be insensitive to the modeling of the surrounding protein, as indicated by the quite small dielectric effects on the relative energies. It should also be noted that the overall similarity of the different structures involved in this process makes the expected accuracy in these calculated relative

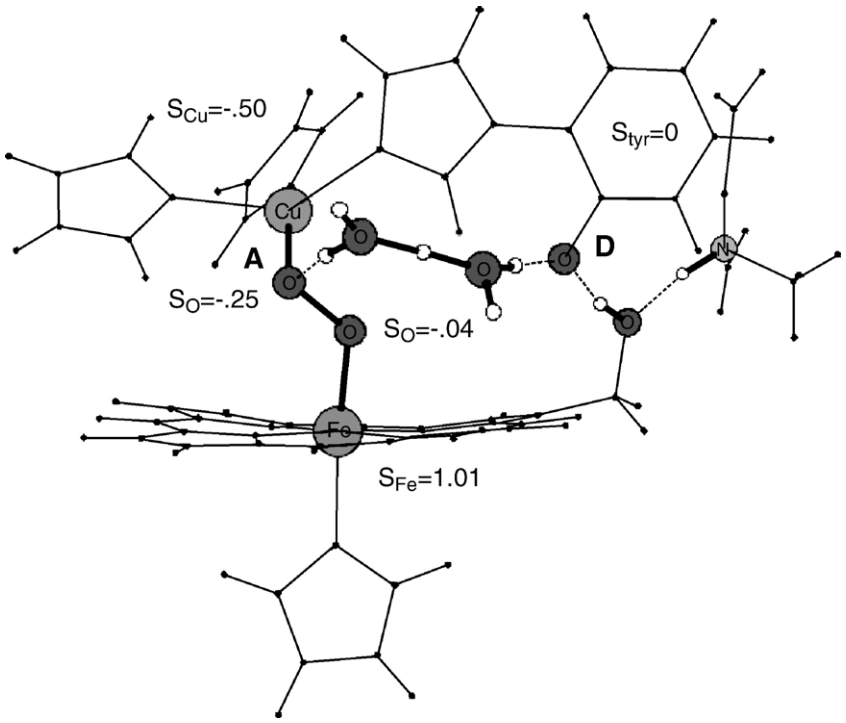

Fig. 6. Intermediate structure in the proton transfer from the tyrosyl hydroxyl donor **D** to the bridging peroxide oxygen acceptor **A**. The most important spin populations are given.

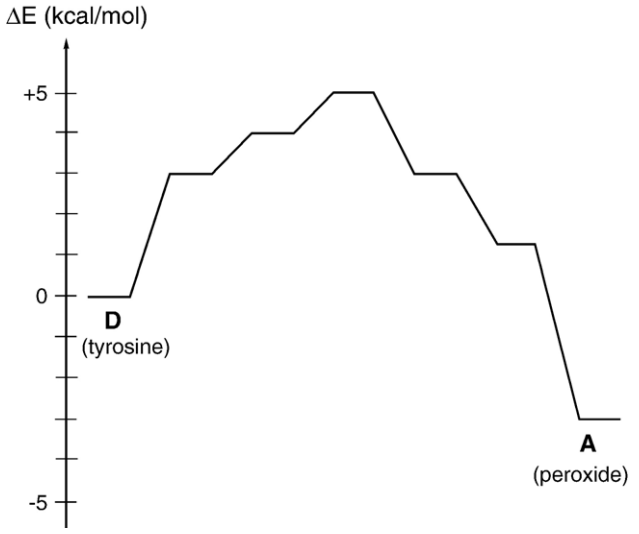

Fig. 7. Potential energy surface for proton transfer from the tyrosyl hydroxyl donor **D** to the bridging peroxide oxygen acceptor **A**. The horizontal lines represent minima, intermediate transition states are not included.

energies higher than the general accuracy of 3–5 kcal/mol mentioned in Introduction.

Another situation when the hydrogen bonding plays an essential role is in the actual O—O bond cleavage step. After the proton has been transferred to the peroxide, the O—O bond can be stretched with a moderate energy increase. In the transition state for the O—O bond cleavage with an O—O bond distance of 2.0 Å, essentially one electron has been transferred from iron to the O—O antibonding σ-orbital. This leads to a shallow minimum for a one-electron bond with Fe(IV) and an O—O bond distance of 2.1 Å. However, when the O—O bond is stretched further the energy goes up and no more electron transfer occurs into the O—O antibonding orbital, as shown in Fig. 8. Again, a proton motion is necessary before an electron transfer can occur. In this case it is found that an essential change has to occur in the hydrogen bonding pattern, such that the hydroxyl group under formation on copper receives, not donates, a hydrogen bond from the water molecule, see Fig. 8. In this new structure, an electron moves from tyrosinate, leaving a neutral tyrosyl radical behind, to the O—O antibonding orbital giving typical spin populations for the Fe(IV)═O and Cu(II)–OH fragments, see Fig. 8. The energy goes down by as much as 9 kcal/mol, and when the freezing of the O—O bond is released the experimentally observed P_M product is formed, with an Fe(IV)═O compound and a tyrosyl radical.

Another interesting observation regarding the importance of protons in the active site of cytochrome oxidase during the O—O bond cleavage is the need for an extra proton in or in the vicinity of the binuclear center. A possible site for such an extra proton could be at or near the Lys319 close to the cross-linked tyrosine. Therefore, in the calculations discussed above, a protonated lysine is included in the model. Without such a protonated lysine the O—O bond cleavage barrier becomes 19.4 kcal/mol [31], which is too high compared to the experimental value of 12.5 kcal/mol, obtained from the life-time of Compound A, using transition state theory [26]. However, if the protonated lysine is included in the model, the barrier decreases to 13.8 kcal/mol, which is in much better agreement with experiment. The main effect of the protonated lysine is to stabilize the negatively charged tyrosinate. It is likely that this extra proton is used in the chemistry or proton translocation, which means that it has to be replaced by a new proton from the inside of the membrane at some point of the catalytic cycle, possibly during the reductive phase.

3.2. Proton transfer connected to the catalytic cycle of CcO

One of the most important remaining questions in bioenergetics is how the protons taken up from the inside of the membrane during the catalytic cycle in cytochrome oxidase are gated towards translocation or chemistry in such a way that the chemical energy is not lost. Many suggestions have been made, some based on structural changes in or near the binuclear center [32–34], and others based on thermodynamic and kinetic preferences [35–39]. It is clear that to solve this problem it is necessary to find a way to elucidate the energetics of all the steps in the chemical process, including the proton translocation, and this is where quantum chemistry can play an important role. Using quantum chemistry, it is in principle quite simple to calculate the relative energies of different states involved in the process. The only obstacle is that it might be difficult to construct good models of the enzyme, since the model cannot be very large if reliable energies should be obtained. In ref. [36] a first attempt was made to use a model of the binuclear center and its closest surrounding to construct a free energy diagram for the whole catalytic cycle of cytochrome oxidase, including the proton translocation, see Fig. 9 for a sketch of the catalytic cycle with observed intermediates. From the results of that model some important conclusions could be drawn. It could first be noted that the overall energetics obtained for the catalytic cycle agree quite well with experimental findings. For example, the reductive part of the cycle (the **O** to **R** steps) was found to be much less exergonic than the oxidative part (the $\mathbf{P_M}$ to **O** steps) [40]. Furthermore, with an extra proton present in the binuclear center during most parts of the cycle no high barriers for proton or electron transfer were obtained [31,36]. An interesting point noted for the model used in the first study was that, when an electron has arrived at the binuclear center, the pK_a value of the heme a_3 propionates, which are believed to function as intermediate sites for the translocated protons, is larger than the pK_a value of the binuclear center. This suggests a mechanism for the proton translocation, where no gate is really needed towards the binuclear center, since it might simply be thermodynamically more favorable to transfer the pumped proton before the chemical protons are transferred to the binuclear center.

To investigate the reliability of the computed energetic results, calculations have been done using a larger model of the binuclear center than the one used in the previous study [36]. The new model is based on a recent crystal structure of the bovine enzyme which includes several water molecules in the vicinity of the active site [41], see Fig. 10. The main extension

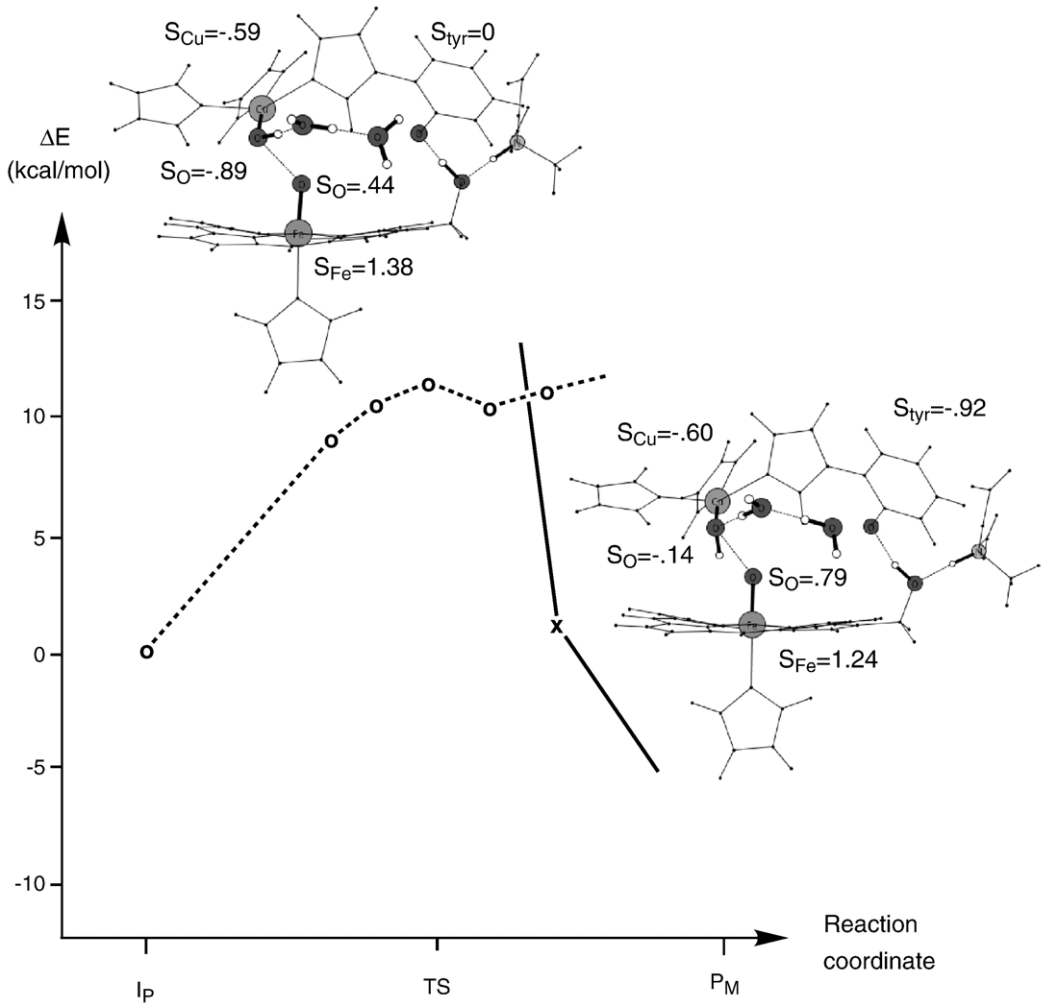

Fig. 8. Energy profile for the O−O bond cleavage step, illustrating the importance of the hydrogen bonding pattern for electron transfer. The most important spin populations are given for two structures with the same O−O bond distance (2.3 Å), but different hydrogen bonding.

of the model is the inclusion of the closest surroundings of the charged substituents on heme a_3, i.e., Arg438 and Asp364, since it was shown for heme a that the corresponding residues have a rather large effect on the calculated Fe(III) electron affinity [31]. A few water molecules from the crystal structure are also included. This model is constructed to improve mainly the calculated redox potentials (electron affinities) and pK_a values (proton affinities) of the binuclear center, which are needed to describe the overall energetics of the catalytic cycle. As it turns out, the values of these proton and electron affinities are quite stable with respect to the model, with the maximum individual change being about 5 kcal/mol. In particular, if one considers the partitioning of the energy gain between the reductive and the oxidative parts of the catalytic cycle, the total shift in going from the previous to the present model is about 5 kcal/mol.

An important result of the previous studies [31,36] was the need for an extra proton in the binuclear center to obtain electron affinities (redox potentials) of similar magnitude for the different steps in the catalytic cycle. It was shown that without this extra proton very large barriers for the electron transfer from heme a to the binuclear center were obtained in three of the four steps [31]. Very similar results are obtained with the present

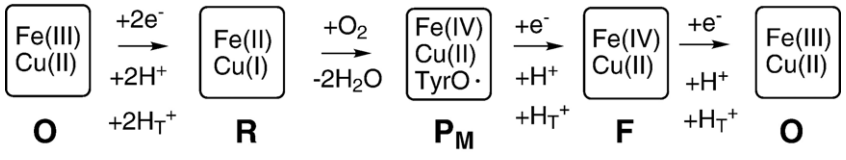

Fig. 9. The catalytic cycle of cytochrome oxidase, showing to most important intermediates. H_T denotes the translocated protons.

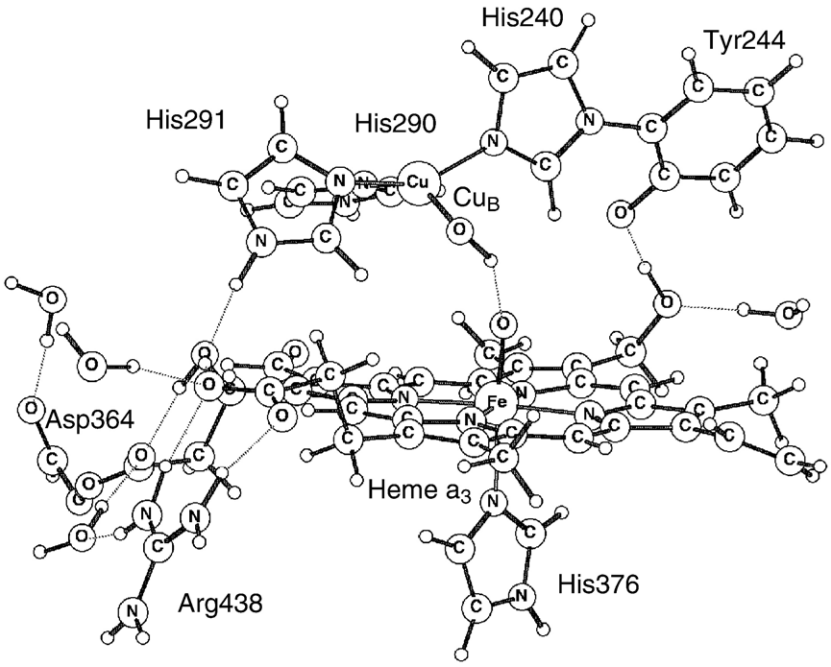

Fig. 10. Model used in the calculation of redox potentials and pK_a values of the binuclear center.

model, with barriers around 60 kcal/mol without the extra proton. There are different possible sources for the extra proton, and in the previous study the extra proton was assumed to be transferred to the binuclear center during the first step in the oxidative part of the cycle [36]. Another possibility discussed in ref. [42], would be to let the first proton go to the ferryl oxygen and keep the tyrosinate unprotonated during the main part of the catalytic cycle. This gives a similar effect as an extra proton in the central part of the binuclear center, and the computed electron affinities are reasonably similar for all steps in the catalytic cycle. Since the tyrosinate oxygen and the ferryl oxygen have similar proton affinities this is an equally likely scheme. In the present discussion it was decided to use a scenario where the tyrosinate is unprotonated until the very end of the catalytic cycle. It should be noted that if there is a connection between the tyrosine and the metal bound oxygens, in the form of one or two water molecules, it is possible that for certain intermediates there is an equilibrium between two different states, one with a neutral tyrosine and one with a tyrosinate and the proton located in the central part of the binuclear center. A shift towards the tyrosine form, could explain the spectroscopic observations that Compound F has a tyrosine and not a tyrosinate [43].

From the calculated redox potentials and pK_a values of all possible intermediates, a free energy profile for the whole catalytic cycle can be constructed, as shown in Fig. 11. The redox potentials and the pK_a values have been parametrized to give a total energy of about 2 eV for the reduction of one molecule of oxygen when the electrons are taken from cytochrome *c*. The parametrization does not affect the relative redoxpotentials nor the relative pK_a values for the different steps. The parametrization is slightly different than the one used in previous studies [31,36], mainly because the presence of the negatively charged tyrosinate in the binuclear center results in lower electron affinities of the binuclear center. Therefore, the redox potential of cytochrome *c* is taken to correspond to a

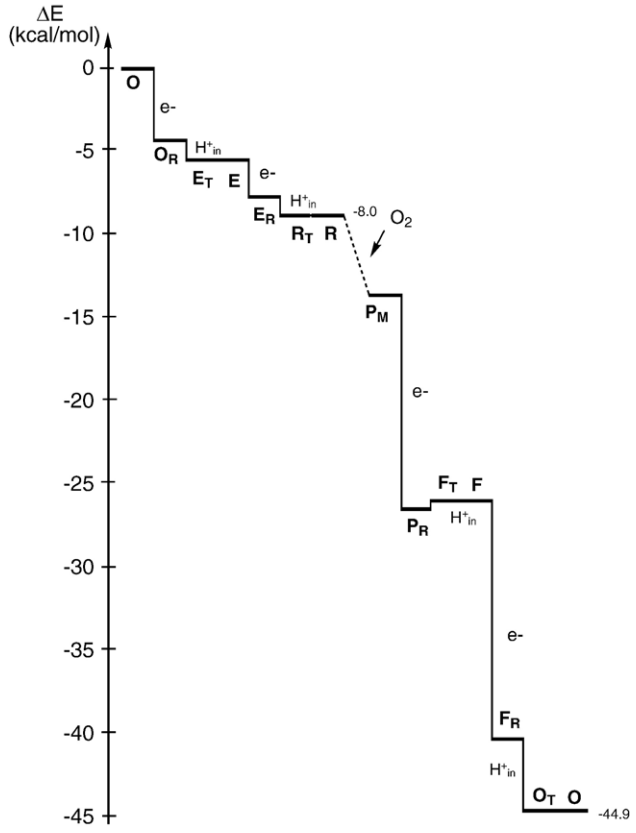

Fig. 11. Energy profile for an entire cycle of cytochrome oxidase in the case without membrane potential.

lower electron affinity of 89 kcal/mol, in parity with the computed value for heme a with unprotonated propionates [36]. In the construction of the profile in Fig. 11 it is furthermore assumed that there is no electrochemical gradient across the membrane. The states with index T are connected to the proton translocation, to be explained and discussed below. The energy profile in Fig. 11 gives a very similar picture for the chemistry occurring in the binuclear center as the previous studies. There are no, or only very low, barriers for the uptake of protons and electrons, and very clearly the reductive part of the cycle (**O** to **R**) is much less exergonic than the oxidative one ($\mathbf{P_M}$ to **O**). The latter result is in accord with experimental observations [40].

The most interesting energy profile, though, is one where there is an electrochemical gradient across the membrane, and where the energy cost for proton translocation is included. For this purpose some kind of description of the translocation mechanism is needed. As was mentioned above, the previous study [36] suggested a mechanism where the translocated protons are actually taken up first, due to high pK_a values of the pumpsite (the propionates) after the electron transfer to the binuclear center. As was discussed later [31] it is quite difficult to construct a model that gives reliable proton affinities (pK_a values) for the pumpsite, which is assumed to be at or near the heme a_3 propionates, since this region has many charged groups and many flexible water molecules. The largest possible model gave a pK_a value only slightly larger for the pumpsite than for the binuclear center [31]. Taking the uncertainty in the calculations into account, the only conclusion on this part that can safely be made is that, after the electron has arrived at the binuclear center, the pumpsite has a pK_a value that is similar to the one in the binuclear center. If the pK_a is somewhat larger at the pumpsite, the mechanism suggested in [36] can be valid, and if the pK_a is somewhat smaller at the pumpsite a gate mechanism switching between the pumpsite and the binuclear center has to be present. The aim of the present discussion is to describe the overall energetics of the catalytic cycle including the proton translocation, not the actual translocation mechanism. Therefore, it is enough to assume that the pumpsite has the same proton affinity as the binuclear center when the electron has arrived. Small discrepancies will only give small fluctuations in the energy profile, which does not affect the conclusions. In the construction of the energy profiles in Figs. 11 and 12 it is assumed that after the electron has arrived at the binuclear center, a proton is transferred to the pumpsite, giving rise to the states with index T. In the next state, the chemical proton is transferred to the binuclear site and the translocated proton is expelled from the pumpsite to the outside of the membrane due to the electrostatic repulsion. With no gradient across the membrane the T state and the following one have the same energy. With a gradient present, the two states differ by the cost of moving a proton across the membrane. The energy profile in Fig. 12 is constructed under the assumption that the electrochemical gradient corresponds to 4.6 kcal/mol (200 mV), and the redox centers of the binuclear center are located one third of the distance from the outside.

The energy profile in Fig. 12 should be read in the following way. The steps labeled e^- correspond to electron transfer to the

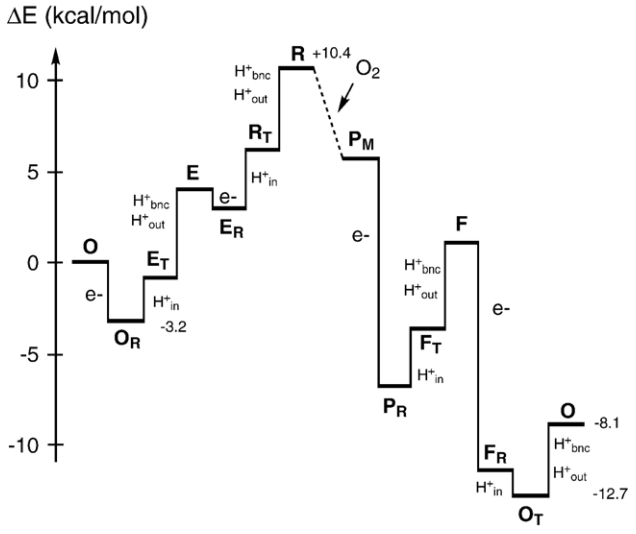

Fig. 12. Energy profile for an entire catalytic cycle of cytochrome oxidase in the case with a membrane potential.

binuclear center, and with the present parameterization all four electron transfer steps are exergonic, also with the gradient present. The steps labeled H^+_{in} correspond to the uptake of a proton to the pumpsite. Here the protonation of the pumpsite is put equal in energy to the protonation of the binuclear center. Most of these steps become somewhat endergonic in the present parametrization. A different choice of parametrization will shift the energy between the electron and proton transfer steps, but the total energy gain and the general features of the profile will stay essentially the same. The steps labeled H^+_{bnc}, H^+_{out}, correspond to proton pumping, i.e., uptake of a proton to the binuclear center and expulsion of the proton at the pumpsite to the outside of the membrane. These steps are always endergonic by the energy of the electrochemical gradient, with the present assumption for the pumpsite energy. In comparison to the previously published energy profile with a gradient present [36], the main features are the same, even if the details differ. There are no prohibitively high barriers due to endergonic electron or proton transfer. As discussed above, only a small part of the exergonicity of the O_2 reduction is gained in the reductive part of the catalytic cycle, and this means that when the gradient is present and protons are being pumped, the reductive part becomes endergonic, as can be seen in Fig. 12. Since the following steps are exergonic, it would not matter with an endergonic part of the catalytic cycle, as long as the cycle is driven by the exergonic part, and as long as the endergonic part does not lead to too high barriers.

The energy profiles shown here only include the energetics of proton and electron uptake, not eventual barriers for the proton motion, and in particular the barrier for the O—O bond cleavage step is not included. The O—O bond cleavage starts from Compound A, which is formed when **R** binds the O_2 molecule, a process which is only slightly exergonic, say by one kcal/mol. From experiment it is known that the O—O bond cleavage barrier is 12.5 kcal/mol relative to Compound A [26], which means that the total barrier for the O—O bond cleavage would be more than 25 kcal/mol relative to the lowest preceding

point ($\mathbf{O_T}$ in the previous cycle). This shows that Compound R is too high in energy, and that when the full gradient has developed, the energy in the reductive half-cycle is not enough for proton pumping, using the present results. It is not likely that this result is caused by inaccuracy in the calculations, and it should be noted that the same conclusion is reached on the basis of titration experiments [40]. Since full proton translocation actually occurs during enzyme turnover, it must be concluded that there is some mechanism present for storing the energy between the half-cycles, a mechanism that is not described by the present models.

4. Conclusions

In this minireview, it has been shown how quantum chemistry can be used to describe proton transfer in biochemical systems, using mainly ribonucleotide reductase (RNR) and cytochrome *c* oxidase (CcO) as examples. In both enzymes, several types of proton transfer processes take place. It is found that in RNR all different proton transfer steps are rather strongly coupled to, and also concerted with electron transfers, with the most strongly coupled case described as a hydrogen atom transfer (HAT). In CcO, on the other hand, proton and electron transfer do not occur concertedly. Instead the coupling between electron and proton transfer appear in such a way that the proton transfer is either triggered by a preceding electron transfer process, or a particular proton motion has to occur to make a succeeding electron transfer possible.

References

[1] R.I. Cukier, D.G. Nocera, Proton-coupled electron transfer, Annu. Rev. Phys. Chem. 49 (1998) 337–369.

[2] S. Hammes-Schiffer, Theoretical perspectives on proton-coupled electron transfer reactions, Acc. Chem. Res. 34 (2001) 273–281.

[3] A.A. Stuchebrukhov, Electron transfer reactions coupled to proton translocation. Cytochrome oxidase, proton pumps, and biological energy transduction, J. Theor. Comp. Chem. 2 (2003) 91–118.

[4] B.-M. Sjöberg, Structure of ribonucleotide reductase from *Escherichia coli*, in: F. Eckstein (Ed.), Nucleic Acids and Molecular Biology, vol. 9, DMJ Lilley, Springer Verlag, 1995, pp. 192–221.

[5] A. Jordan, P. Reichard, Ribonucleotide reductase, Annu. Rev. Biochem. 67 (1998) 71–98.

[6] J. Stubbe, W.A. van der Donk, Protein radicals in enzyme catalysis, Chem. Rev. 98 (1998) 705–762.

[7] P.E.M. Siegbahn, L. Eriksson, F. Himo, M. Pavlov, Hydrogen atom transfer in ribonucleotide reductase (RNR), J. Phys. Chem. 102 (1998) 10622–10629.

[8] G.T. Babcock, The oxygen-evolving complex in photosystem II as a metallo-radical enzyme, in: P. Mathis (Ed.), Photosynthesis from Light to Biosphere, vol. 2, Kluwer, Dordrecht, 1995, p. 209.

[9] R.B. Gennis, How does cytochrome oxidase pump protons? Proc. Natl. Acad. Sci. U. S. A. 95 (1998) 12747–12749.

[10] S. Ferguson-Miller, G. Babcock, Heme/copper terminal oxidases, Chem. Rev. 96 (1996) 2889–2907.

[11] H. Michel, J. Behr, A. Harrenga, A. Kannt, Cytochrome *c* oxidase: structure and spectroscopy, Annu. Rev. Biophys. Biomol. Struct. 27 (1998) 329–356.

[12] J.E. Morgan, M.I. Verkhovsky, G. Palmer, M. Wikström, On the role of the P_R intermediate in the reaction of cytochrome *c* oxidase with O_2, Biochemistry 40 (2001) 6882–6892.

[13] A.D. Becke, Density-functional exchange-energy approximation with correct asymptotic behavior, Phys. Rev. A38 (1988) 3098–3100;
A.D. Becke, A new mixing of Hartree–Fock and local density-functional theories, J. Chem. Phys. 98 (1993) 1372–1377;
A.D. Becke, Density-functional thermochemistry: III. The role of exact exchange, J. Chem. Phys. 98 (1993) 5648–5652.

[14] P.E.M. Siegbahn, Mechanisms of metalloenzymes studied by quantum chemical methods, Q. Rev. Biophys. 36 (2003) 91–145.

[15] M. Ekberg, M. Sahlin, M. Eriksson, B.M. Sjöberg, Two conserved tyrosine residues in protein R1 participate in an intermolecular electron transfer in ribonucleotide reductase, J. Biol. Chem. 271 (1996) 20655–20659.

[16] A. Ehrenberg, P. Reichard, Electron spin resonance of the iron-containing protein B2 from ribonucleotide reductase, J. Biol. Chem. 247 (1972) 3485–3588.

[17] A.J. Skulan, T.C. Brunold, J. Baldwin, L. Saleh, J.M. Bollinger Jr., E.I. Solomon, Nature of the peroxo intermediate of the W48F/D84E ribonucleotide reductase variant: implications for O-2 activation by binuclear non-heme iron enzymes, J. Am. Chem. Soc. 126 (2004) 8842–8855.

[18] W.-G. Han, T. Liu, T. Lovell, L. Noodleman, Active site structure of class I ribonucleotide reductase intermediate X: a density functional theory analysis of structure, energetics, and spectroscopy, J. Am. Chem. Soc. 127 (2005) 15778–15790.

[19] K.N. Ferreira, T.M. Iverson, K. Maghlaoui, J. Barber, S. Iwata, Architecture of the photosynthetic oxygen-evolving center, Science 303 (2004) 1831–1838.

[20] P.E.M. Siegbahn, M. Lundberg, Hydroxide instead of bicarbonate in the structure of the oxygen evolving complex, J. Inorg. Biochem. (submitted for publication).

[21] V. Pelmenschikov, K.-B. Cho, P.E.M. Siegbahn, Class I ribonucleotide reductase revisited: the effect of removing a proton on Glu441, J. Comp. Chem. 25 (2004) 311–321.

[22] M. Lundberg, P.E.M. Siegbahn, Quantifying the effects of the self-interaction error in DFT—When do the delocalized states appear? J. Chem. Phys. 122 (2005) 224103-1-9.

[23] F. Himo, P.E.M. Siegbahn, A very stable substrate radical relevant for class I ribonucleotide reductase (RNR), J. Phys. Chem., B 104 (2000) 7502–7509.

[24] M. Wikström, Proton pump coupled to cytochrome *c* oxidase in mitochondria, Nature 266 (1977) 271–273.

[25] D.A. Proshlyakov, M.A. Pressler, G.T. Babcock, Dioxygen activation and bond cleavage by mixed valence cytochrome *c* oxidase, Proc. Natl. Acad. Sci. U. S. A. 95 (1998) 8020–8025.

[26] M. Karpefors, P. Ädelroth, A. Namslauer, Y. Zhen, P. Brzezinski, Formation of the, peroxy, intermediate in cytochrome *c* oxidase is associated with internal proton/hydrogen transfer, Biochemistry 39 (2000) 14664–14669.

[27] D.A. Proshlyakov, M.A. Pressler, C. DeMaso, J.F. Leykam, D.L. DeWitt, G.T. Babcock, Oxygen activation and reduction in respiration: involvement of redox-active tyrosine 244, Science 290 (2000) 1588–1591.

[28] S. Yoshikawa, K. Shinzawa-Itoh, R. Nakashima, R. Yaono, E. Yamashita, N. Inoue, M. Yao, M.J. Fei, C.P. Libeu, T. Mizushima, H. Yamaguchi, T. Tomizaki, T. Tsukihara, Redox-coupled crystal structural changes in bovine heart cytochrome *c* oxidase, Science 280 (1998) 1723–1729.

[29] M.R.A. Blomberg, P.E.M. Siegbahn, G.T. Babcock, M. Wikström, Modeling cytochrome oxidase—A quantum chemical study of the O—O bond cleavage mechanism, J. Am. Chem. Soc. 122 (2000) 12848–12858.

[30] M.R.A. Blomberg, P.E.M. Siegbahn, M. Wikström, A metal-bridging mechanism for O—O bond cleavage in cytochrome *c* oxidase, Inorg. Chem. 42 (2003) 5231–5243.

[31] P.E.M. Siegbahn, M.R.A. Blomberg, Quantum chemical models of O_2 bond cleavage and proton pumping in cytochrome oxidase, in: M. Wikström (Ed.), Biophysical and Structural Aspects of Bioenergetics, Royal Society of Chemistry, Cambridge, UK, 2005, pp. 99–122.

[32] J.E. Morgan, M.I. Verkhovsky, M. Wikström, The histidine cycle; a new model for proton translocation in the respiratory heme-copper oxidase, J. Bioenerg. Biomembranes 26 (1994) 599–608;
M. Wikström, J.E. Morgan, M.I. Verkhovsky, On the mechanism of proton translocation by respiratory enzyme, J. Bioenerg. Biomembranes 30 (1998) 139–145;

M. Wikström, Mechanism of proton translocation by cytochrome *c* oxidase: a new four-stroke histidine cycle, Biochim. Biophys. Acta 44827 (2000) 1–11.

[33] M. Wikström, M.I. Verkhovsky, G. Hummer, Water-gated mechanism of proton translocation by cytochrome *c* oxidase, Biochim. Biophys. Acta 1604 (2003) 61–65.

[34] P. Brzezinski, G. Larsson, Redox-driven proton pumping by heme-copper oxidases, Biochim. Biophys. Acta 1605 (2003) 1–13.

[35] H. Michel, The mechanism of proton pumping by cytochrome *c* oxidase, Proc. Natl. Acad. Sci. U. S. A. 95 (1998) 12819–12824;
H. Michel, Cytochrome *c* oxidase: catalytic cycle and mechanism of proton pumping—A discussion, Biochemistry 38 (1999) 15129–15140;
M. Ruitenberg, A. Kannt, E. Bamberg, K. Fendler, H. Michel, Reduction of cytochrome *c* oxidase by a second electron leads to proton translocation, Nature 417 (2002) 99–102.

[36] P.E.M. Siegbahn, M.R.A. Blomberg, M.L. Blomberg, A theoretical study of the energetics of proton pumping and oxygen reduction in cytochrome oxidase, J. Phys. Chem., B 107 (2003) 10946–10955.

[37] D.M. Popovic, A.A. Stuchebrukhov, Electrostatic study of the proton pumping mechanism in bovine heart cytochrome *c* oxidase, J. Am. Chem. Soc. 126 (2004) 1858–1871.

[38] D.M. Popovic, A.A. Stuchebrukhov, Proton pumping mechanism and catalytic cycle of cytochrome *c* oxidase: coulomb pump model with kinetic gating, FEBS Lett. 566 (2004) 126–130.

[39] D.M. Popovic, J. Quenneville, A.A. Stuchebrukhov, DFT/electrostatic calculations of pK_a values in cytochrome *c* oxidase, J. Phys. Chem., B 109 (2005) 3616–3626.

[40] M. Wikström, Cytochrome *c* oxidase: 25 years of the elusive proton pump, Biochim. Biophys. Acta 1655 (2004) 241–247.

[41] T. Tsukihara, K. Shimokata, Y. Katayama, H. Shimada, K. Muramoto, H. Aoyama, M. Mochizuki, K. Shinzawa-Itoh, E. Ymashita, M. Yao, Y. Ishimura, S. Yoshikawa, The low-spin heme of cytochrome *c* oxidase as the driving element of the proton-pumping process, Proc. Natl. Acad. Sci. U. S. A. 100 (2003) 15304–15309.

[42] P.E.M. Siegbahn, M.R.A. Blomberg, Important roles of tyrosines in photosystem II and cytochrome oxidase, Biochim. Biophys. Acta 1655 (2004) 45–50.